

Fu-Qiang Zhang · Hai-Shun Wu · Yuan-Yuan Xu ·
Yong-Wang Li · Haijun Jiao

Structure and stability of neutral polyoxometalate cages: $(\text{Mo}_2\text{O}_6)_m$ ($m=1-13$)

Received: 4 March 2005 / Accepted: 2 December 2005 / Published online: 11 May 2006
© Springer-Verlag 2006

Abstract The structure and stability of neutral polyoxometalate cages $(\text{Mo}_2\text{O}_6)_m$ ($m=1-13$) have been computed systematically. These neutral cages can be viewed topologically as polyhedra containing triangles (f_3) and squares (f_4). The relative stability of these polyhedra is associated with the location and separation of the f_3 . The initial stable isomers were preselected by the number of shared triangle edges (N_{33}), and the predicted stability was validated further at the GGA-PW91/DND level of density function theory with the fine quality of mesh size. For large clusters, the square neighbor signature (P_{4444}), which is similar to the hexagon neighbor rule for fullerene, becomes more applicable. The calculated disproportionation energies indicate that Mo_6O_{18} (O_h , Lindqvist), $\text{Mo}_{12}\text{O}_{36}$ (O_h , α Keggin), $\text{Mo}_{18}\text{O}_{54}$ (D_{3h} , Wells–Dawson) and $\text{Mo}_{24}\text{O}_{72}$ (O_h) cages have enhanced stability.

Keywords POM · Neutral cage · Keggin · Stability · DFT

Introduction

Molybdenum and tungsten polyoxometalates (POM) constitute an extreme variety of compounds in number

Dedicated to Professor Dr. Paul von Ragué Schleyer on the occasion of his 75th birthday.

F.-Q. Zhang · Y.-W. Li · H. Jiao
The State Key Laboratory of Coal Conversion,
Institute of Coal Chemistry, Chinese Academy of Sciences,
Taiyuan, People's Republic of China

F.-Q. Zhang · H.-S. Wu (✉) · Y.-Y. Xu
Department of Chemistry, Shanxi Normal University,
Linfen, People's Republic of China
e-mail: wuhs@dns.sxtu.edu.cn

H. Jiao
Leibniz-Institut für Organische Katalyse
an der Universität Rostock eV,
Albert-Einstein-Strasse 29a,
18059 Rostock, Germany

and diversity [1]. Their interesting and potentially valuable physical and chemical properties have made impact on catalysis, biology, medicine, and materials science [2–4]. Besides the typical architectures, such as the Lindqvist [5] anion $[\text{M}_6\text{O}_{19}]^{2-}$ ($\text{M}=\text{Mo}, \text{W}$), Tungstate Y [6] anion $[\text{M}_{10}\text{O}_{32}]^{x-}$, the Keggin [7] anion $[\text{XM}_{12}\text{O}_{40}]^{y-}$, and the Wells–Dawson [8] anion $[\text{X}_2\text{M}_{18}\text{O}_{62}]^{y-}$ ($\text{X}=\text{Al}, \text{P}, \text{S}, \text{As}$, etc), as well as a huge number of their derivatives, many other isopoly and heteropoly structures have resulted in an unmatched structural variety.

Many POM can be considered as supramolecular species with identifiable host cages and encapsulated guests [9]. One important hypothesis referred to as the *clathrate* model suggests that a Keggin anion can be viewed as an $[\text{XO}_4]^{y-}$ anion encapsulated in a neutral $\text{M}_{12}\text{O}_{36}$ cage [10]. Poblet et al. [11] have verified this model for a set of Keggin anions with density functional theory calculations. Recently, this model was also found to be applicable to Wells–Dawson anions [12]. Thus, the clathrate model enables us to study a wider range of properties of POM, despite their intrinsic multiformality, complexity, and the arbitrary encapsulated guest anions.

The shape of the framework and the composition of the metal define the POM properties. Most of the typical POM structures exhibit interpenetrating closed loops, formed by the metal center and the bridging oxygen atoms. Based on this idea, a structure stability index was developed by Nomiya and Miwa [13], and they proposed the analogy of closed loops of this type to macrocyclic π -bonding systems. However, this stability index cannot be applied to $[\text{PM}_{12}\text{O}_{40}]^{3-}$, as indicated by Bridgeman et al. [14]. With graph theory and topology as bases, King [15] studied the aromaticity of POM and pointed out that the closed loops might play a significant role in electron transfer processes. In particular, upon analyzing a set of α/β Keggin anions, Poblet et al. [11] found that the intrinsic stability of the neutral $\alpha\text{-M}_{12}\text{O}_{36}$ cage over the β one controls stability.

Knowledge of the structure and stability of metal-oxide clusters offers valuable insight into the physical and chemical properties of condensed matter [16]. Because of the properties of similar discrete fragments of metal oxide

structures of definite sizes and shapes, these species can be viewed as soluble metal-oxide analogues and are therefore of special interest as models for the reactions and properties of oxides. [10, 17] Despite the abundant experimental data and considerable activity in POM research in the last 30 years [18], the basic structural properties still need to be rationalized systematically.

On the basis of the clathrate model and density functional theory computations, the stability of all neutral Keggin ($M_{12}O_{36}$) and Wells–Dawson ($M_{18}O_{54}$) ($M=Mo$, W) cages has been investigated systematically [19]. These cages can be viewed topologically as polyhedra, and their stabilities obey the isolated triangle rule (ITR), e.g., the more the isolated triangles, the more stable the isomer. As an extension, we report our results of all neutral POM cages ($Mo_2O_6)_m$ ($m=1-13$). It is found that these cages obey the ITR rule, which is similar to the isolated square rule (ISR) [20] for boron nitride (BN) inorganic fullerenes and isolated pentagon rule (IPR) [21] for carbon fullerenes. Therefore, neutral POM cages can be considered as inorganic fullerenes.

Computational methods

All calculations were performed within density functional theory using the DMol³ program available from the Materials Studio package of Accelrys [22]. The initial structures obtained were relaxed and adjusted to their highest symmetry using the Visualizer build-in. For selecting more stable isomers, the initial structures were sorted by the number of the shared triangle edges (N_{33}) [19] and then optimized fully using the local density approximation with the Vosko–Wilk–Nusair [23] parameters, double numerical basis set (DN) and the *coarse*-quality mesh size for numerical integration. The five most stable structures obtained for each ($Mo_2O_6)_m$ were further refined using the generalized gradient corrected (GGA) functional by Perdew and Wang (PW91) [24], the DND basis set (the DN set augmented by a set of d polarization functions), and the *fine*-quality mesh size for numerical integration. Effect core potentials were used for metallic elements throughout the calculations. The tolerances of the final energy convergence, gradient, and the displacement convergence were 2×10^{-5} a.u., 4×10^{-4} a.u./Å, and 5×10^{-4} Å, respectively. The real space cutoff of atomic orbitals was set at 5.5 Å. Increasing the convergence criteria to 2×10^{-7} a.u., 4×10^{-6} a.u./Å, and 5×10^{-6} Å, changes the total electronic energies of the two most stable $Mo_{26}O_{78}$ isomers in D_{2d} and D_2 symmetries by no more than 0.004 kcal mol⁻¹, and their relative energies by less than 0.007 kcal mol⁻¹.

The quality of the method used (GGA-PW91/DND) has been validated on the basis of the nearly perfect agreement between the computed and estimated α/β stability, as well as the structural parameters of $[AlW_{12}O_{40}]^{5-}$ [25]. For example, the computed α/β stability of $[AlW_{12}O_{40}]^{5-}$ of 2.02 kcal mol⁻¹ agrees very well with the estimated 2.1 ± 0.5 kcal mol⁻¹ by experiment [26], and the available theoretical data (2.37 kcal mol⁻¹) [27]. The computed

structural parameters also agree very well with the available X-ray data.

Results and discussion

Design principle

Due to the structural complexity of POM, it is difficult to take all conditions into consideration. In this paper, only the type I structure of Pope [28], with tractable M/O ratio (1:3), closed shell configuration, and *ideal* four-connected metal structures, was considered [29].

The Euler equation (Eq. 1) [30] holds for every convex polyhedron, where v is the number of vertices, f the number of faces, and e the number of edges. For a polyhedron of a POM cage in which each metal center and the connecting oxygen atoms can be considered topologically as a vertex, each vertex is connected with four edges and there are many possible kinds of coexisting faces, such as triangle (f_3), square (f_4), pentagon (f_5), and hexagon (f_6) faces. Their relationships are expressed in Eqs. 2, 3, and 4. Because of the absence of larger face types such as f_5 and f_6 , Eq. 6 can be simplified to Eqs. 7 and 8 for small clusters of Mo _{v} ($v\leq 26$). All topological structures can be generated easily using the plantri [31] program (which realizes the sphere quadrangulation algorithms) or the modified fullerene spiral algorithms [32].

$$v + f = e + 2 \quad (1)$$

$$4v = 2e \quad (2)$$

$$f = \sum f_i \quad (3)$$

$$\sum (i \times f_i) = 2e \quad (4)$$

Considering Eqs. 1, 2, 3, and 4, we obtained Eqs. 5 and 6

$$f = v + 2 \quad (5)$$

$$f_3 - \sum (i - 4)f_i = 8 \quad (i \geq 4) \quad (6)$$

$$f_3 = 8 \quad (7)$$

$$f_4 = v - 6 \quad (8)$$

Structure and stability

Figure 1 shows the most stable $(\text{Mo}_2\text{O}_6)_m$ structures obtained, and some selected bond distances are given in Table 1. Free from the influence of the encapsulated anions, the structural parameters obtained are very close to the available X-ray data. For $\text{Mo}_{12}\text{O}_{36}/\text{O}_h$ and $\text{Mo}_{18}\text{O}_{54}/\text{O}_h$, the calculated bond length of the metal-bridging oxygen atom ($\text{Mo}-\text{O}_b$) and Mo–Mo distances are in the scope of the experimental data. Similar to previous theoretical studies [11, 12, 33], the bond length of the metal terminal oxygen ($\text{M}-\text{O}_t$) is overestimated by about 0.03 Å on average, and Guo et al. [34] have attributed this to the absence of crystal environment, and the largest deviation of the nonbonded Mo–Mo distances in $\text{Mo}_6\text{O}_{18}/\text{O}_h$ can be attributed to the absence of the central O^{2-} .

The stability of the most stable $(\text{Mo}_2\text{O}_6)_m$ clusters was tested using the binding energy (ΔE_m) on the basis of the dimer structure $[(\text{Mo}_2\text{O}_6)_m, m=1]$, as defined in Eq. 9. The same method has been used to estimate the most stable isomers and the effect of cage sizes of $(\text{AlN})_x$ clusters [35], $(\text{BN})_x$ clusters [36], $(\text{MeAlO})_x$ cages [37], and Al_x clusters [38]. The computed data are given in Table 2 and plotted in Fig. 2. One can see clearly that the binding energy increases strongly for $m \leq 6$, and this change is mainly attributed to the reduced strain with increased cage size. [36] However, the binding energy hardly changes for $m \geq 6$, indicating that the strain contribution is nearly constant. However, detailed analysis shows that cluster with $m=6$ has

Table 1 Selected distances (in Ångstrom, interval values) of the most stable $(\text{Mo}_2\text{O}_6)_m$ ($m=1-13$) cages

$(\text{Mo}_2\text{O}_6)_m/\text{sym}$	Mo– O_t	Mo– O_b	Mo–Mo
$\text{Mo}_2\text{O}_6/\text{C}_{2v}$	1.719–1.720	1.935	2.857
$\text{Mo}_4\text{O}_{12}/\text{C}_{4v}$	1.719	1.911	3.619
$\text{Mo}_6\text{O}_{18}/\text{O}_h$	1.703	1.933	3.458
Expt ^a	1.67–1.69	1.90–1.94	3.28–3.29
$\text{Mo}_8\text{O}_{24}/\text{D}_{4d}$	1.702	1.931–1.938	3.397–3.690
$\text{Mo}_{10}\text{O}_{30}/\text{D}_2$	1.703	1.922–1.956	33.462–3.838
$\text{Mo}_{12}\text{O}_{36}/\text{O}_h$	1.701	1.923	3.693
Expt ^b	1.67–1.69	1.85–1.97	3.42–3.73
$\text{Mo}_{14}\text{O}_{42}/\text{D}_{2d}$	1.700–1.703	1.914–1.933	3.503–3.745
$\text{Mo}_{16}\text{O}_{48}/\text{D}_{4d}$	1.702	1.917–1.924	3.690–3.692
$\text{Mo}_{18}\text{O}_{54}/\text{D}_{3h}$	1.701–1.703	1.917–1.926	3.634–3.750
Expt ^c	1.672–1.689	1.902–2.024	3.432–3.764
$\text{Mo}_{20}\text{O}_{60}/\text{D}_2$	1.701–1.704	1.907–1.937	3.668–3.826
$\text{Mo}_{22}\text{O}_{66}/\text{D}_{2d}$	1.701–1.703	1.903–1.942	1.684–1.765
$\text{Mo}_{24}\text{O}_{72}/\text{O}_h$	1.702	1.915–1.923	3.762–3.763
$\text{Mo}_{26}\text{O}_{78}/\text{D}_4$	1.700–1.702	1.886–1.942	3.666–3.776

^aX-ray data from [51]

^bX-ray data from [52]

^cX-ray data from [53]

enhanced stability, and this is also found for $(\text{AlN})_{12}$ [35], $(\text{BN})_{12}$ [36], and $(\text{MeAlO})_{12}$ [37].

$$\Delta E_m = E(\text{Mo}_2\text{O}_6) - E_m/m \quad (9)$$

Fig. 1 The most stable $(\text{Mo}_2\text{O}_6)_m$ clusters ($m=1-13$)

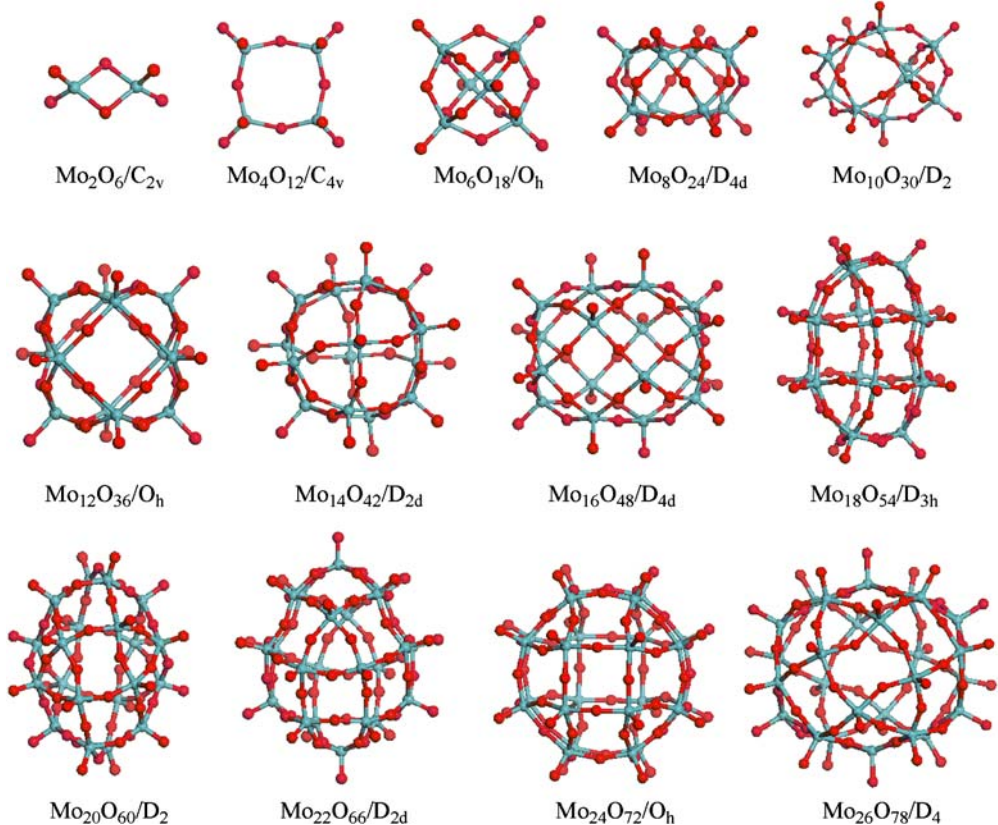


Table 2 Total electronic energies (E_{tot} , a.u.) and relative energies (kcal mol⁻¹) of the most stable ($(\text{Mo}_2\text{O}_6)_m$ ($m=1-13$) cages

$(\text{Mo}_2\text{O}_6)_m/\text{sym}$	$E_{\text{tot}}^{\text{a}}$	ΔE_m^{b}	$\Delta^2 E_m^{\text{c}}$	Isomers ^d	Isomers ^e
$\text{Mo}_2\text{O}_6/C_{2v}$	-588.4325	0.0		0	0
$\text{Mo}_4\text{O}_{12}/C_{4v}$	-1,176.9502	27.2	-11.0	0	0
$\text{Mo}_6\text{O}_{18}/O_h$	-1,765.5030	43.7	10.9	0	0
$\text{Mo}_8\text{O}_{24}/D_{4d}$	-2,354.0208	46.3	2.2	0	0
$\text{Mo}_{10}\text{O}_{30}/D_2$	-2,942.5316	47.1	-8.5	2	0
$\text{Mo}_{12}\text{O}_{36}/O_h$	-3,531.0696	50.4	13.1	5	1
$\text{Mo}_{14}\text{O}_{42}/D_{2d}$	-4,119.5660	49.0	-6.9	8	0
$\text{Mo}_{16}\text{O}_{48}/D_{4d}$	-4,708.0844	49.8	0.6	12	2
$\text{Mo}_{18}\text{O}_{54}/D_{3h}$	-5,296.6008	50.2	2.7	25	3
$\text{Mo}_{20}\text{O}_{60}/D_2$	-5,885.1086	49.9	-3.4	30	3
$\text{Mo}_{22}\text{O}_{66}/D_{2d}$	-6,473.6271	50.4	-1.9	51	5
$\text{Mo}_{24}\text{O}_{72}/O_h$	-7,062.1516	51.1	8.1	76	12
$\text{Mo}_{26}\text{O}_{78}/D_4$	-7,650.6502	50.4		109	17

^aAt GGA-PW91/DND/Fine

^bBinding energy ΔE_m per Mo_2O_6 unit (Eq. 8)

^cDisproportionation energy (Eq. 9)

^dTotal number of all the possible topological isomers (not including ringlike isomers)

^eNumber of isolated-triangle rule isomers in parenthesis

Insight into the enhanced stability can be gained from the second difference in energy $\Delta^2 E_m$ in Eq. 10, where E_{m+1} , E_{m-1} , and E_m are the energies of $(\text{Mo}_2\text{O}_6)_{m+1}$, $(\text{Mo}_2\text{O}_6)_{m-1}$, and $(\text{Mo}_2\text{O}_6)_m$. Because Eq. 10 can be considered as a disproportionation reaction of a molecule into two fragments, the calculated reaction energy ($\Delta^2 E_m$) can reveal the relative stability of the cluster, i.e., a positive value (endothermic) for enhanced stability toward fragmentation and a negative value (exothermic) for instability. The same method has been used to estimate the stability of $(\text{AlN})_x$ clusters, [35] $(\text{BH})_x^{2-}$ cages, [39] and Al_x clusters [38]. As given in Table 2 and shown in Fig. 3, the relationship between $\Delta^2 E_m$ and m alternates with increasing cage sizes, where Mo_6O_{18} (Lindqvist), $\text{Mo}_{12}\text{O}_{36}$ (Keggin), and $\text{Mo}_{24}\text{O}_{72}$ stand out as *stable* cages. To a lesser extent, $\text{Mo}_{18}\text{O}_{54}$ (Wells–Dawson) also appears to be

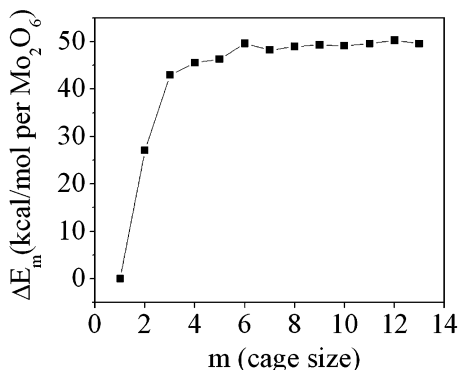


Fig. 2 Binding energy ΔE_m per Mo_2O_6 unit as a function of the cage size (m)

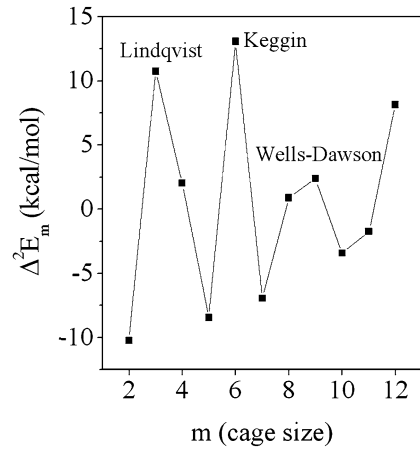


Fig. 3 Disproportionation energy $\Delta^2 E_m$ as a function of the cage size (m)

stable. The largest disproportionation energy of 13.1 kcal mol⁻¹ identifies the neutral α -Keggin cage $\text{Mo}_{12}\text{O}_{36}$ as the most stable cluster. It is noteworthy that the anions of Mo_6O_{12} , $\text{Mo}_{12}\text{O}_{36}$, and $\text{Mo}_{18}\text{O}_{54}$ are known experimentally, but that the anions of $\text{Mo}_{24}\text{O}_{72}$ are unknown.

$$\Delta^2 E_m = (E_{m+1} + E_{m-1})/2 - E_m \quad (10)$$

The stability of a given POM cage depends on the structure and bonding environment. Assigning certain coefficients to the $\{\text{O}_4\text{Mo}=\text{O}\}$ unit in different bonding environments is an effective means for predicting energies. To understand the relationship between the stability and structure of POM, a least-squares fit is done using the bonding environment index, as suggested by Ziegler [37]. For simplification, each pyramidal $\{\text{O}_4\text{Mo}=\text{O}\}$ unit¹ (corresponding to the octahedron $\{\text{O}_5\text{Mo}=\text{O}\}$ in the POM anions) is extracted as a point, and there are six possible points (P_{4444} , P_{4443} , P_{4343} , P_{4433} , P_{4333} , and P_{3333}) according to their surrounding number of f_4 and f_3 , respectively, e.g., P_{4443} for the point with three f_4 and one f_3 around, and P_{4343} for point surrounded by two f_4 and two f_3 alternatively.

The fit gives the energy expression in Eq. 11 for $(\text{MoO}_3)_n$ cages with $\{\text{O}_4\text{Mo}=\text{O}\}$ units at the GGA-PW91/DND/FINE level. $E(v)$ is the total electronic energy, and n (equal to $m/2$) is the number of the $\{\text{MoO}_3\}$ units. The root-mean-square deviation of this fit for the total energy is 21.2 kcal mol⁻¹. The fit has been checked on all stable cages in Fig. 3 and the largest differences are found for

¹ Because each bridged-oxygen linked by two metal atoms, so in fact each pyramid reduced to one $\{\text{MO}_3\}$ unit in average.

Mo_6O_{18} and $\text{Mo}_{24}\text{O}_{78}$ with about 33.9 kcal mol⁻¹ (<0.03%). The significant energy deviation can be

attributed to the large difference of local bonding environment, as discussed later.

$$E(v, \text{a.u.}) = -294.2550v - [0.9331P_{4443} + 0.2854P_{4343} + (-1.1118)P_{4444} + (-1.3305)P_{4433} + (-2.6286)P_{4333} + (-4.5031)P_{3333}] \times 10^{-3}. \quad (11)$$

Moreover, it must be noticed that the coefficients pertaining to each specific point provide a means to gauge the stability of a particular environment [37]. The more positive the coefficient, the more stable the environment. Hence, the stability is, in decreasing order, $P_{4443} > P_{4343} > P_{4444} > P_{4433} > P_{3333}$. Thus, P_{4443} and P_{4343} are more stable types, while P_{3333} and P_{4333} are less stable types. It is clearly seen that P_{3333} and P_{4333} exhibit a large amount of ring strain and destabilize the structure. Along with the IPR [21] for carbon fullerenes or ISR [20] for BN inorganic fullerenes, these neutral POM cages obey the ITR.

However, there exists a large difference between the predicted and calculated energies, and this can be attributed to the fact that in this simple model the local bonding environment is neglected. For example, the peripheral MMM angles of the P_{4444} in small cages, such as the most stable $\text{Mo}_{14}\text{O}_{42}$ (which shares the similar skeleton with $([\text{PMo}_{12}\text{O}_{40}(\text{VO})_2]^{5-})$ [40] reaches 57.2°, while in large clusters, such as $\text{Mo}_{26}\text{O}_{78}$, the MMM angle of P_{4444} is 87.3°. This difference in structural parameters will result in the large deviation of the energy fit.

Beside the isolated arrangement of triangles, the squares of the polyhedron should have environments as similar as possible for spreading the steric strain evenly. This is similar to the hexagon neighbor rule (HNR) [41] of fullerenes. Here, we use the number of P_{4444} to depict simply the square neighbor signatures. Taking the first ten most stable isomers of $\text{Mo}_{22}\text{O}_{66}$ and $\text{Mo}_{24}\text{O}_{72}$ as examples (Table 3), besides the general trend on the stability obeying the ITR, the number of P_{4444} also correlates obviously with the stability. For example, the most stable isomer **1** of $\text{Mo}_{22}\text{O}_{66}$ is the exclusive one, not only with the largest triangles isolation ($N_{33}=0$) but also with the most isolated squares ($P_{4444}=0$); while isomers (**2–10**), with $P_{4444}=2–3$, are all higher in energy. For $\text{Mo}_{24}\text{O}_{72}$, the most stable isomers **11** and **12** are the only ones with $N_{33}=0$ and $P_{4444}=0$, the third most stable isomer **13**, with $P_{4444}=2$ and $N_{33}=0$, is higher in energy, while other isomers with $P_{4444}>2$ are much higher in energy. Thus, the square neighbor rule (SNR) is applicable in selecting the first few stable isomers, and for big clusters, it shows obvious superiority than N_{33} . Thus, the more reliable method is combining P_{4444} with N_{33} . For the Keggin cages ($\text{Mo}_{12}\text{O}_{36}$), the most stable cage is the α isomer with $N_{33}=0$, while the β isomer with $N_{33}=3$ is higher in energy by 8.0 kcal mol⁻¹ [19]. For the Wells–Dawson cage ($\text{Mo}_{18}\text{O}_{54}$), the most stable cage is the α isomer with

$N_{33}=0$, while second most stable cage in C_{2v} symmetry with $N_{33}=2$ is higher in energy by 1.8 kcal mol⁻¹. It is also noteworthy that with increased cage sizes, these isomers become very close in energy and their relative stability and cannot be estimated simply by such rules.

The analogy with fullerenes can be perused further. For example, the α -Keggin cage ($\text{Mo}_{12}\text{O}_{36}$) with $f_3=8$ and $f_4=6$ is the first structure composed only of perfectly isolated triangles, which corresponds to C_{60} without pentagon adjacency ($f_5=12$ and $f_6=20$) and $(\text{BN})_{12}$ without square adjacency ($f_4=6$ and $f_6=8$). The second example is the Lindqvist cage (Mo_6O_{18}) composed only of triangles ($f_3=8$), and the analogous fullerene counterpart is C_{20} with only pentagons ($f_5=12$) [42] and the $(\text{BN})_n$ counterpart is $(\text{BN})_4$ with only squares ($f_4=6$) [20]. The next analogue is $\text{Mo}_{16}\text{O}_{48}$, which obeys the ITR ($f_3=8$ and $f_4=10$), and the counterpart is C_{70} following the IPR ($f_5=12$ and $f_6=25$), and $(\text{BN})_{15}$ is following the ISR ($f_4=8$ and $f_6=11$) [20]. In addition, no

Table 3 Total electronic energies (E_{tot} , a.u.) and relative energies (E_{rel} , kcal mol⁻¹) of the first ten stable of $\text{Mo}_{22}\text{O}_{66}$ and $\text{Mo}_{24}\text{O}_{72}$ isomers

	P_{4444}	N_{33}	$E_{\text{tot}}^{\text{a}}$	$E_{\text{rel}}^{\text{a}}$
$\text{Mo}_{22}\text{O}_{66}$				
1 / D_{2d}	0	0	-6,473.6271	0.0
2 / D_4	2	0	-6,473.6144	8.0
3 / C_2	2	0	-6,473.6125	9.2
4 / C_{2v}	2	0	-6,473.6116	9.7
5 / C_1	2	1	-6,473.6100	10.7
6 / C_s	2	0	-6,473.6095	11.0
7 / C_2	2	2	-6,473.6081	11.9
9 / C_2	2	1	-6,473.6018	15.9
8 / C_2	2	2	-6,473.6006	16.6
10 / C_2	3	2	-6,473.5978	18.4
$\text{Mo}_{24}\text{O}_{72}$				
11 / D_{4d}	0	0	-7,062.1516	0.0
12 / D_{4h}	0	0	-7,062.1516	0.0
13 / C_2	2	0	-7,062.1247	16.9
14 / C_2	4	2	-7,062.1225	18.3
15 / C_1	3	1	-7,062.1198	20.0
16 / D_2	4	0	-7,062.1184	20.8
17 / C_1	3	1	-7,062.1170	21.7
18 / C_1	4	1	-7,062.1167	21.9
19 / C_2	4	2	-7,062.1136	23.8
20 / C_2	4	1	-7,062.1128	24.4

^aAt GGA-PW91/DND/Fine

Table 4 Total electronic energies (E_{tot} , a.u.) and relative energies (E_{rel} to the most stable one, kcal mol $^{-1}$) of the second most stable $(\text{Mo}_2\text{O}_6)_m$ ($m=2-13$) clusters

$(\text{Mo}_2\text{O}_6)_m/\text{sym}$	E_{tot}	$E_{\text{rel}}^{\text{a},\text{b}}$
$\text{Mo}_4\text{O}_{12}/C_{2v}$	-1,176.9486	1.0
$\text{Mo}_6\text{O}_{18}/D_{3d}$	-1,765.4347	42.9
$\text{Mo}_8\text{O}_{24}/C_2$	-2,353.9357	53.4
$\text{Mo}_{10}\text{O}_{30}/D_{4h}$	-2,942.5211	6.6
$\text{Mo}_{12}\text{O}_{36}/C_{3v}$	-3,531.0568	8.0
$\text{Mo}_{14}\text{O}_{42}/C_2$	-4,119.5534	7.9
$\text{Mo}_{16}\text{O}_{48}/C_2$	-4,708.0795	3.1
$\text{Mo}_{18}\text{O}_{54}/C_{2v}$	-5,296.5972	1.8
$\text{Mo}_{20}\text{O}_{60}/D_{2d}$	-5,885.1081	0.3
$\text{Mo}_{22}\text{O}_{66}/D_4$	-6,473.6144	8.0
$\text{Mo}_{24}\text{O}_{72}/D_{4d}$	-7,062.1516	0.0
$\text{Mo}_{26}\text{O}_{78}/C_s$	-7,650.6353	9.3

^aAt GGA-PW91/DND/Fine

^bRelative energies to the most stable isomers in Table 1

perfect ITR POM structures can exist for $12 < m < 16$, while no IPR fullerene structures can exist for $60 < m < 70$, and no ISR (BN)_x structures can exist for $12 < x < 15$ [20]. On the basis of the similarity in stability and structure between POMs and fullerene as well as BN fullerene, this kind of neutral shell can be considered as inorganic fullerene.

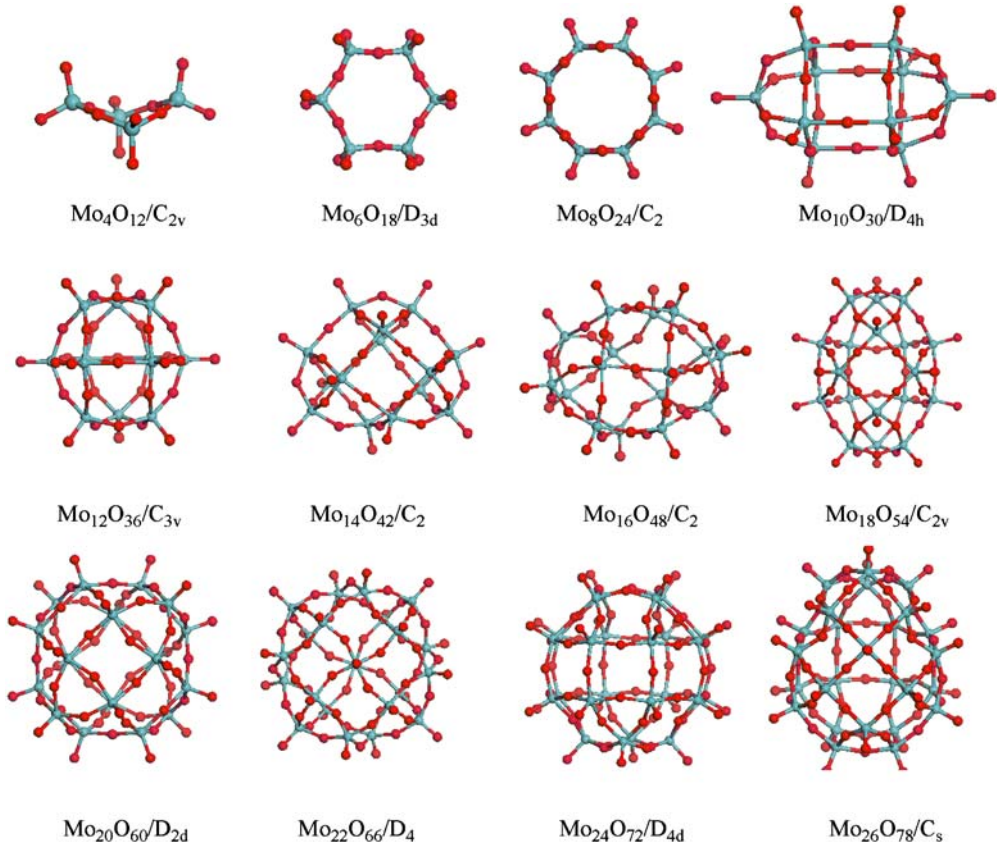
It is noteworthy that, similar to fullerene [43] and BN fullerene [35, 44], the energy differences between these isomers are small. For simplicity, only the second most

stable isomers are discussed in this paper; the optimized structures are shown in Fig. 4 and the energies are given in Table 4. Apart from $\text{Mo}_{4}\text{O}_{12}/D_{2d}$, $\text{Mo}_{18}\text{O}_{54}/C_{2v}$, $\text{Mo}_{20}\text{O}_{60}/D_{2d}$, and $\text{Mo}_{24}\text{O}_{72}/D_{4d}$, which are very close in energy to the most stable isomers (1.0, 1.8, 0.3, and 0.0 kcal mol $^{-1}$, respectively), all the other isomers are higher in energy than the most stable isomers (Table 1).

As pointed out previously, this topological analysis can also be used for clusters with large sizes (big or giant) with f_5 , and the relationship between f_5 and f_3 is $f_3 = f_5 + 8$ (Eq. 6 is changed to $f_3 - f_5 = 8$). For example, Presyssler's anion ($[\text{NaP}_5\text{W}_{30}\text{O}_{110}]^{14-}$) [45] has a neutral cage of $\text{M}_{30}\text{O}_{90}$, and it can be considered as a polyhedron with $f_3=10$, $f_4=20$, and $f_5=2$. The giant keplerates $\{\text{Mo}_{102}\}$ [46], $\{\text{Mo}_{72}\text{Fe}_{30}\}$ [47], and $\{\text{Mo}_{132}\}$ [48], in striking similarity with C_{60} , can be viewed as derivatives of $\text{M}_{60}\text{O}_{180}$ (I_h , $f_3=20$, $f_4=30$, and $f_5=12$). They were described as $\{\text{Mo}_{60}\}(\text{pentagon})_{12}(\text{linker})_{30}$ for $\{\text{Mo}_{102}\}$ and $\{\text{Mo}_{72}\text{Fe}_{30}\}$, as well as $\{\text{Mo}_{60}\}(\text{pentagon})_{12}(\text{linker})_{60}$ for $\{\text{Mo}_{132}\}$ by Müller [46] recently. Accordingly, $\{\text{Mo}_{75}\text{V}_{20}\}$ [49] as derivatives of $\text{M}_{30}\text{O}_{90}$ (I_h , $f_3=20$, $f_4=0$, and $f_5=12$) can be viewed as $\{\text{Mo}_{30}\}(\text{Mo}_6)(\text{Mo}_5)$ [46]. Within the topological analysis, all these clusters have perfectly arranged triangles and, therefore, obey the ITR.

Apart from the discussion above, note that our topological analysis and computations are on the basis of the clathrate model. However, POM cages are seldom empty, and the interaction between the host and guest exists. It has often been noted that the assembly of the flexible and versatile metal oxide compounds is probably

Fig. 4 The second most stable $(\text{Mo}_2\text{O}_6)_m$ ($m=2-13$) clusters



determined by the shape and symmetry of small guest molecule [50]. Although there are several factors competing in the control of the stability of POMs [11], the sizes of host and guest must be compatible for a chemical interaction with the formation of pseudo-octahedral metal coordination. For example, considered as a stable cage, the POM of the $\text{Mo}_{24}\text{O}_{72}$ (O_h) cage is still unknown; one of the problems is the appropriate guest to be encapsulated and to be stabilized in solution, as Pope et al. rationalized [45]. Combining chemical rationality and topological stability, the WD structures are more similar to C_{70} than the $\text{Mo}_{16}\text{O}_{48}$ as the second ITR, as shown in Fig. 2. Because of the unavailability of appropriate guests, the anions of some stable neutral cages cannot be formed experimentally.

Conclusions

Using sphere quadrangulation algorithms or modified fullerene spiral algorithms, all possible cage isomers of $(\text{Mo}_2\text{O}_6)_m$ ($m=1-13$) structures have been generated. Their relative stabilities were estimated qualitatively by using the number of the shared triangle cages (N_{33}) and calculated at the GGA-W91/DND level of density functional theory with the fine quality of mesh size. Like the HNR of fullerene, the SNR was also found useful for selecting the most stable isomers. The most stable neutral cages of $(\text{Mo}_2\text{O}_6)_m$ ($m=3-13$) that mimic the IPR of fullerene and ISR of inorganic fullerene (BN_x) are found to obey the ITR. Based on the disproportionation energy, the Mo_6O_{12} , $\text{Mo}_{12}\text{O}_{36}$, and $\text{Mo}_{18}\text{O}_{54}$ cages have enhanced stability, and they correspond to the neutral cages of the Lindqvist, Keggin, and Wells–Dawson anions, respectively. Among them, the neutral the α -Keggin $\text{Mo}_{12}\text{O}_{36}$ is the first ITR isomer and represents the most stable cage of these clusters. The Wells–Dawson ($\text{Mo}_{18}\text{O}_{54}$) cage represents the second ITR structure, which corresponds to C_{70} as the second IPR cage of fullerene. Therefore, neutral cages of $(\text{Mo}_2\text{O}_6)_m$ ($m=3-13$) can be viewed as inorganic fullerenes.

Acknowledgements The work was supported by Chinese Academy of Sciences and the National Natural Science Foundation China (20471034).

References

- (a) Pope MT (1983) *Heteropoly and isopoly oxometalates*. Springer, Berlin Heidelberg New York; (b) Pope MT, Müller A (1991) *Angew Chem Int Ed Engl* 30:34–48
- Pope MT, Müller A (1994) Polyoxometalates: from platonic solids to anti-retroviral activity. Kluwer, Dordrecht, The Netherlands
- Hill CL, Weeks MS, Schinazi RF (1990) *J Med Chem* 22:2767–2772
- (a) Hill CL (1998) *Chem Rev* 98:1–390 (Special issue on polyoxometalates); (b) Chen YG, Gong J, Qu LY (2004) *Coord Chem Rev* 248:245–260
- (a) Gouzerh P, Jeannin Y, Proust A, Robert F (1989) *Angew Chem Int Ed Engl* 28:1363–1364; (b) Lindqvist I (1952) *Ark Kemi* 5:247–250
- (a) Fuchs J, Hartl H, Schiller W, Gerlach U (1976) *Acta Crystallogr B* 32:248; (b) Chemseddine A, Sanchez C, Livage J, Launay JP, Fournier M (1984) *Inorg Chem* 23:2609–2613; (c) Duncan DC, Hill CL (1996) *Inorg Chem* 35:5828–5835
- Kegg JF (1933) *Nature* 131:908–909
- (a) Dawson B (1953) *Acta Crystallogr* 6:113–126; (b) D’Amour H (1976) *Acta Crystallogr C* 32:729–740
- Müller A (1991) *Nature* 352:115–115
- Day VW, Klempener WG (1985) *Science* 228:533–541
- (a) López X, Maestre JM, Bo C, Poblet JM (2001) *J Am Chem Soc* 123:9571–9576; (b) Maestre JM, López X, Bo C, Poblet JM, Casao-Pastor N (2001) *J Am Chem Soc* 123:3749–3758; (c) Maestre JM, López X, Poblet JM (2002) *Inorg Chem* 41:1883–1888; (d) Poblet JM, López X, Bo C (2003) *Chem Soc Rev* 32:297–308; (f) Rohmer MM, Bénard M, Blaudeau JP, Maestre JM, Poblet JM (1998) *Coord Chem Rev* 178:1019–1049
- (a) López X, Bo C, Poblet JM (2002) *J Am Chem Soc* 124:12574–12582; (b) López X, Bo C, Poblet JM (2003) *Inorg Chem* 42:2634–2638
- (a) Nomiya K, Miwa M (1984) *Polyhedron* 3:341–346; (b) Nomiya K, Miwa M (1984) *Polyhedron* 4:89–95; (c) Nomiya K, Miwa M (1985) *Polyhedron* 4:675–679; (d) Nomiya K, Miwa M (1985) *Polyhedron* 4:1407–1412; (e) Nomiya K (1987) *Polyhedron* 6:309–314
- Bridgeman AJ, Cavigliasso G (2003) *J Phys Chem A* 107:6613–6621
- (a) King RB (2001) *J Chem Inf Comput Sci* 41:517–526; (b) King RB (1992) *J Chem Inf Comput Sci* 32:42–47; (c) King RB (1991) *Inorg Chem* 30:4437–4440
- Sambrano JR, Andres J, Beltran A, Sensato F, Longo E (1998) *Chem Phys Lett* 287:620–626
- Baker LCW (1961) *Advances in the chemistry of coordination compounds*. Macmillan, New York, p 604
- Dividson ER (2000) *Chem Rev* 100:351–818 (special issue on computational transition metal chemistry)
- Zhang FQ, Wu HS, Cao DB, Zhang XM, Li YW, Jiao H (2005) *J Mol Struct Theochem* 755:119–126
- Fowler PW, Heine T, Mitchell D, Schmidt R, Seifert G (1996) *J Chem Soc Faraday Trans* 92:2197–2201
- (a) Kroto HW (1987) *Nature (Lond)* 329:529–531; (b) Schmalz TG, Seitz WA, Klein DJ, Hite GE (1988) *J Am Chem Soc* 110:1113–1127
- (a) Delley B (1990) *J Chem Phys* 92:508–517; (b) Delley B (2000) *J Chem Phys* 113:7756–7764 (DMol³ is available as part of Materials Studio.)
- Vosko SH, Wilk L, Nusair M (1980) *Can J Phys* 58:1200–1211
- Wang Y, Perdew JP (1991) *Phys Rev B* 44:13298–13307
- Zhang FQ, Wu HS, Qin XF, Li YW, Jiao, H (2005) *J Mol Struct Theochem* 755:113–117
- Weinstock IA, Cowan JJ, Barbuzzi EMG, Zeng H, Hill CL (1999) *J Am Chem Soc* 121:4608–4617
- López X, Poblet JM (2004) *Inorg Chem* 43:6863–6865
- Pope MT (1972) *Inorg Chem* 11:1973–1974
- (a) Friedrichs OD, Dress AWM, Hudson DH, Klinowski J, Mackay AL (1999) *Nature* 400:644–647; (b) Friedrichs OD, Dress AWM, Müller A, Pope MT (1993) *Mol Eng* 3:9–28
- (a) Coxeter HSM (1961) *Introduction to geometry*. Wiley, New York; (b) Cerari M, Cucinella S (1987) The chemistry of inorganic homo and heterocycles. In: Haiduc I, Sowerby DB (eds) Academic, New York, pp 167–190
- Brinkman G, McKay B (2001) Plantri and fullgen. <http://www.mathematik.uni-bielefeld.de/~senkel/CAGE/contents.html>
- Manolopoulos DE, May JC, Down SE (1991) *Chem Phys Lett* 181:105–111

33. (a) Bridgeman AJ (2004) *Chem Eur J* 10:2935–2941; (b) Bridgeman AJ, Cavigliasso G (2003) *J Phys Chem A* 107:6613–6621; (c) Bridgeman AJ (2003) *Chem Phys* 287:55–69; (d) Bridgeman AJ, Cavigliasso G (2002) *Inorg Chem* 41:1761–1770; (e) Bridgeman AJ, Cavigliasso G (2002) *Chem Phys* 279:143–159; (f) Bridgeman AJ, Cavigliasso G (2002) *Inorg Chem* 41:3500–3507; (g) Bridgeman AJ, Cavigliasso G (2002) *J Chem Soc Dalton Trans* 2244–2249
34. Guo YR, Pan QJ, Wei YD, Li ZH, Li X (2004) *J Mol Struct Theochem* 676:55–64
35. Wu HS, Zhang FQ, Xu XH, Zhang CJ, Jiao H (2003) *J Phys Chem A* 107:204–209
36. Seifert G, Fowler PW, Mitchell D, Porezag D, Frauenheim T (1997) *Chem Phys Lett* 268:352–358
37. Zurek E, Woo TK, Ziegler T (2001) *Inorg Chem* 40:361–370
38. Lloyd LD, Johnston RL (1998) *Chem Phys* 236:107–121
39. Schleyer PvR, Najafian K, Mebel AM (1998) *Inorg Chem* 37:6765–6772; see also Schleyer PvR, Najafian K (1998) *Inorg Chem* 37:3454–3470
40. Chen Q, Hill CL (1996) *Inorg Chem* 35:2403–2405
41. (a) Raghavachari K (1992) *Chem Phys Lett* 190:397–400; (b) Achiba Y, Fowler PW, Mitchell D, Zerbetto F (1998) *J Phys Chem A* 102:6835–6841
42. Prinzbach H, Weller A, Landenberger P, Wahl F, Worth J, Scott LT, Gelmont M, Olevano D, Issendorff BV (2000) *Nature* 407:60–63
43. (a) Cioslowski J, Rao N, Moncrieff D (2000) *J Am Chem Soc* 122:8265–8270; (b) Zhao X, Slanina Z, Goto H (2004) *J Phys Chem A* 108:4479–4484; (c) Wu HS, Xu XH, Jiao H (2004) *J Phys Chem A* 108:3813–3816
44. (a) Strout DL (2004) *Chem Phys Lett* 383:95–98; (b) Strout DL (2001) *J Phys Chem A* 105:261–263
45. (a) Alizadeh MH, Harmalker SP, Jeannin Y, Martin-Frère J, Pope MT (1985) *J Am Chem Soc* 107:2662–2669; (b) Dickman MH, Gama GJ, Kim KC, Pope MT (1996) *J Clust Sci* 7: 567–583
46. Müller A, Kögerler P, Dress AWM (2001) *Coord Chem Rev* 222:193–218
47. Müller A, Das SK, Kögerler P, Böggel H, Schmidtmann M, Trautwein AX, Schünemann V, Krickemeyer E, Preetz W (2000) *Angew Chem Int Ed Engl* 39:3414–3417
48. Müller A, Krickemeyer E, Böggel H, Schmidtmann M, Preetz W, Peters F (1998) *Angew Chem Int Ed Engl* 37:3359–3363
49. Müller A, Koop M, Böggel H, Schmidtmann M, Peters F (1999) *Chem Commun* 1885–1886
50. (a) Müller A, Reuter H, Dillinger S (1995) *Angew Chem Int Ed Engl* 34:2328–2361; (b) Müller A, Rohlfing R, Krickemeyer E, Böggel H (1993) *Angew Chem Int Ed Engl* 32:909–912; (c) Müller A, Krickemeyer E, Penk M, Rohlfing R, Armatage A, Böggel H (1991) *Angew Chem Int Ed Engl* 30:1674–1677
51. (a) Dahlstrom P, Zubie J, Neaves B, Dilworth JR (1982) *Cryst Struct Commun* 11:463–469; (b) Garner CD, Giwkaderm NC, Mabbs FE, McPhail AT, Miller RW, Onan KD (1978) *J Chem Soc Dalton Trans* 1582–1589
52. Bi LH, Wang EB, Xu L, Huang RD (2000) *Inorg Chim Acta* 305:163–171
53. Neier R, Trojanowski C, Mattes R (1995) *J Chem Soc Dalton Trans* 2521–2528